frontiers in Physiology

ORIGINAL RESEARCH
published: 24 August 2021
doi: 10.3389/fphys.2021.704518

# Mechanical Stimulation-Induced Calcium Signaling by Piezo1 Channel Activation in Human Odontoblast Reduces Dentin Mineralization

*Mayumi Matsunaga[1,2], Maki Kimura[1†], Takehito Ouchi[1†], Takashi Nakamura[3], Sadao Ohyama[1], Masayuki Ando[1], Sachie Nomura[1], Toshifumi Azuma[3], Tatsuya Ichinohe[2] and Yoshiyuki Shibukawa[1*]*

[1]Department of Physiology, Tokyo Dental College, Tokyo, Japan, [2]Department of Dental Anesthesiology, Tokyo Dental College, Tokyo, Japan, [3]Department of Biochemistry, Tokyo Dental College, Tokyo, Japan

OPEN ACCESS

**Edited by:**
*Timothy C. Cox, University of Missouri–Kansas City, United States*

**Reviewed by:**
*Gehoon Chung, Seoul National University, South Korea*
*Zhi Chen, Wuhan University, China*

***Correspondence:**
*Yoshiyuki Shibukawa*
*yshibuka@tdc.ac.jp*

*[†]These authors have contributed equally to this work*

**Specialty section:**
*This article was submitted to Craniofacial Biology and Dental Research, a section of the journal Frontiers in Physiology*

**Received:** *03 May 2021*
**Accepted:** *03 August 2021*
**Published:** *24 August 2021*

**Citation:**
*Matsunaga M, Kimura M, Ouchi T, Nakamura T, Ohyama S, Ando M, Nomura S, Azuma T, Ichinohe T and Shibukawa Y (2021) Mechanical Stimulation-Induced Calcium Signaling by Piezo1 Channel Activation in Human Odontoblast Reduces Dentin Mineralization. Front. Physiol. 12:704518. doi: 10.3389/fphys.2021.704518*

Odontoblasts play critical roles in dentin formation and sensory transduction following stimuli on the dentin surface. Exogenous stimuli to the dentin surface elicit dentinal sensitivity through the movement of fluids in dentinal tubules, resulting in cellular deformation. Recently, Piezo1 channels have been implicated in mechanosensitive processes, as well as $Ca^{2+}$ signals in odontoblasts. However, in human odontoblasts, the cellular responses induced by mechanical stimulation, Piezo1 channel expression, and its pharmacological properties remain unclear. In the present study, we examined functional expression of the Piezo1 channel by recording direct mechanical stimulation-induced $Ca^{2+}$ signaling in dentin matrix protein 1 (DMP-1)-, nestin-, and dentin sialophosphoprotein (DSPP)-immunopositive human odontoblasts. Mechanical stimulation of human odontoblasts transiently increased intracellular free calcium concentration ($[Ca^{2+}]_i$). Application of repeated mechanical stimulation to human odontoblasts resulted in repeated transient $[Ca^{2+}]_i$ increases, but did not show any desensitizing effects on $[Ca^{2+}]_i$ increases. We also observed a transient $[Ca^{2+}]_i$ increase in the neighboring odontoblasts to the stimulated cells during mechanical stimulation, showing a decrease in $[Ca^{2+}]_i$ with an increasing distance from the mechanically stimulated cells. Application of Yoda1 transiently increased $[Ca^{2+}]_i$. This increase was inhibited by application of $Gd^{3+}$ and Dooku1, respectively. Mechanical stimulation-induced $[Ca^{2+}]_i$ increase was also inhibited by application of $Gd^{3+}$ or Dooku1. When Piezo1 channels in human odontoblasts were knocked down by gene silencing with short hairpin RNA (shRNA), mechanical stimulation-induced $[Ca^{2+}]_i$ responses were almost completely abolished. Piezo1 channel knockdown attenuated the number of Piezo1-immunopositive cells in the immunofluorescence analysis, while no effects were observed in Piezo2-immunopositive cells. Alizarin red staining distinctly showed that pharmacological activation of Piezo1 channels by Yoda1 significantly suppressed mineralization, and shRNA-mediated knockdown of Piezo1 also significantly enhanced mineralization. These results suggest that mechanical stimulation predominantly activates intracellular $Ca^{2+}$ signaling *via* Piezo1 channel opening, rather

than Piezo2 channels, and the $Ca^{2+}$ signal establishes intercellular odontoblast-odontoblast communication. In addition, Piezo1 channel activation participates in the reduction of dentinogenesis. Thus, the intracellular $Ca^{2+}$ signaling pathway mediated by Piezo1 channels could contribute to cellular function in human odontoblasts in two ways: (1) generating dentinal sensitivity and (2) suppressing physiological/reactional dentinogenesis, following cellular deformation induced by hydrodynamic forces inside dentinal tubules.

**Keywords: dentin, odontoblast, Piezo channel, mechanosensitive channel, tooth pain, orofacial pain**

## INTRODUCTION

Piezo proteins are large membrane proteins and components of mechanosensitive non-selective cationic channels (Bagriantsev et al., 2014; Beech and Xiao, 2018). Piezo channels are classified into two subtypes: Piezo1 (encoded by the *FAM38A* gene) and Piezo2 (encoded by the *FAM38B* gene; Bagriantsev et al., 2014; Morozumi et al., 2020). In mammals, Piezo1 is mainly expressed in cells with essential mechanosensory functions, such as skin, bladder, kidney, lung, endothelial cells, erythrocytes, and periodontal ligament cells (Bagriantsev et al., 2014; Borbiro and Rohacs, 2017). Piezo1 is required for vascular development, stretch-induced epithelial proliferation, crowdsensing, urinary osmolarity regulation, and neuronal stem cell lineage choice (Beech and Xiao, 2018; Dalghi et al., 2019). In contrast, Piezo2 is prominently expressed in the lung, bladder, dorsal root ganglia, and trigeminal ganglia (Coste et al., 2010; Bagriantsev et al., 2014). Piezo2 is also required for the sensation of touch in the Merkel cells of the skin, proprioception, airway stretch, and respiration (Woo et al., 2014; Chesler et al., 2016; Nonomura et al., 2017).

Odontoblasts have been reported to express Piezo1 and Piezo2 channels (Khatibi Shahidi et al., 2015; Miyazaki et al., 2019). In addition, Piezo1 channels in rat odontoblasts play an essential role in mechanosensory processes as mechanosensitive ion channels and mediate the intracellular $Ca^{2+}$ signaling pathway to release neurotransmitters, establishing neural communication between odontoblasts and the intradental Aδ neurons (Sato et al., 2018). Odontoblast-neuron communication generates action potential on the neurons, resulting in the development of dentinal sensitivity (odontoblast hydrodynamic receptor model; Shibukawa et al., 2015; Sato et al., 2018). However, the detailed functional properties of Piezo1 channel in odontoblasts remain to be clarified. To further investigate the functional expression and pharmacological profiles of Piezo channels and their cellular functions, we examined mechanical stimulation- and ligand-evoked intracellular $Ca^{2+}$ signaling by Piezo channel activation in human odontoblasts. We also investigated the effects of Piezo1 channel knockdown by gene silencing with short hairpin RNA (shRNA) on the direct mechanical stimulation-induced intracellular free $Ca^{2+}$ concentration ($[Ca^{2+}]_i$) increases. In addition, we examined the role of Piezo1 channels during dentinogenesis using mineralizing assays.

## MATERIALS AND METHODS

### Cell Culture

Human odontoblast cells were obtained from a healthy third molar and immortalized by transfection with the human telomerase transcriptase gene (Kitagawa et al., 2007; Ichikawa et al., 2012; Kimura et al., 2016; Kojima et al., 2017). The resulting cells showed mRNA expression of dentin sialophosphoprotein (DSPP), type 1 collagen, alkaline phosphatase, and bone sialoprotein, and exhibited nodule formation by Alizarin red staining in the mineralizing medium (Kitagawa et al., 2007). Note that these cells were immunopositive for odontoblast marker proteins (**Figure 1**). The cells were gifted by Dr. Takashi Muramatsu of Tokyo Dental College, Japan. Human odontoblasts were cultured in basal medium [alpha-minimum essential medium containing 10% FBS, 1% penicillin–streptomycin (Life Technologies, Tokyo, Japan), and amphotericin B (Sigma-Aldrich, St. Louis, MO, United States)] at 37°C in a humidified atmosphere of 5% $CO_2$ for 48 h. The odontoblast suspension was adjusted to a density of $5 \times 10^4$ cells/ml.

### Solutions and Reagents

Standard extracellular solution (standard ECS) containing (in mM) 136 NaCl, 5 KCl, 2.5 $CaCl_2$, 0.5 $MgCl_2$, 10 HEPES, 10 glucose, and 12 $NaHCO_3$ (adjusted to pH 7.4 with Tris) was used as the extracellular solution. A selective pharmacological Piezo1 channel activator, Yoda1 (Syeda et al., 2015), was obtained from Cayman Chemical Company (Ann Arbor, MI, United States). A non-selective mechanosensitive ion channel inhibitor, $GdCl_3$ ($Gd^{3+}$; Ermakov et al., 2010), and a pharmacological competitive antagonist of Yoda1, Dooku1 (Evans et al., 2018), were obtained from R&D Systems, Inc. (Minneapolis, MN, United States). Stock solutions of Yoda1 and Dooku1 were prepared in dimethyl sulfoxide. The other was prepared using ultrapure water (Millipore, MA, United States). Stock solutions were diluted with standard ECS to an appropriate concentration before use.

### Direct Mechanical Stimulation of Single Human Odontoblast

Direct mechanical stimulation (Sato et al., 2015; Shibukawa et al., 2015; Nishiyama et al., 2016) was applied using a fire-polished glass micropipette with a tip diameter of 2–3 μm, which was filled with standard ECS. Micropipettes were pulled

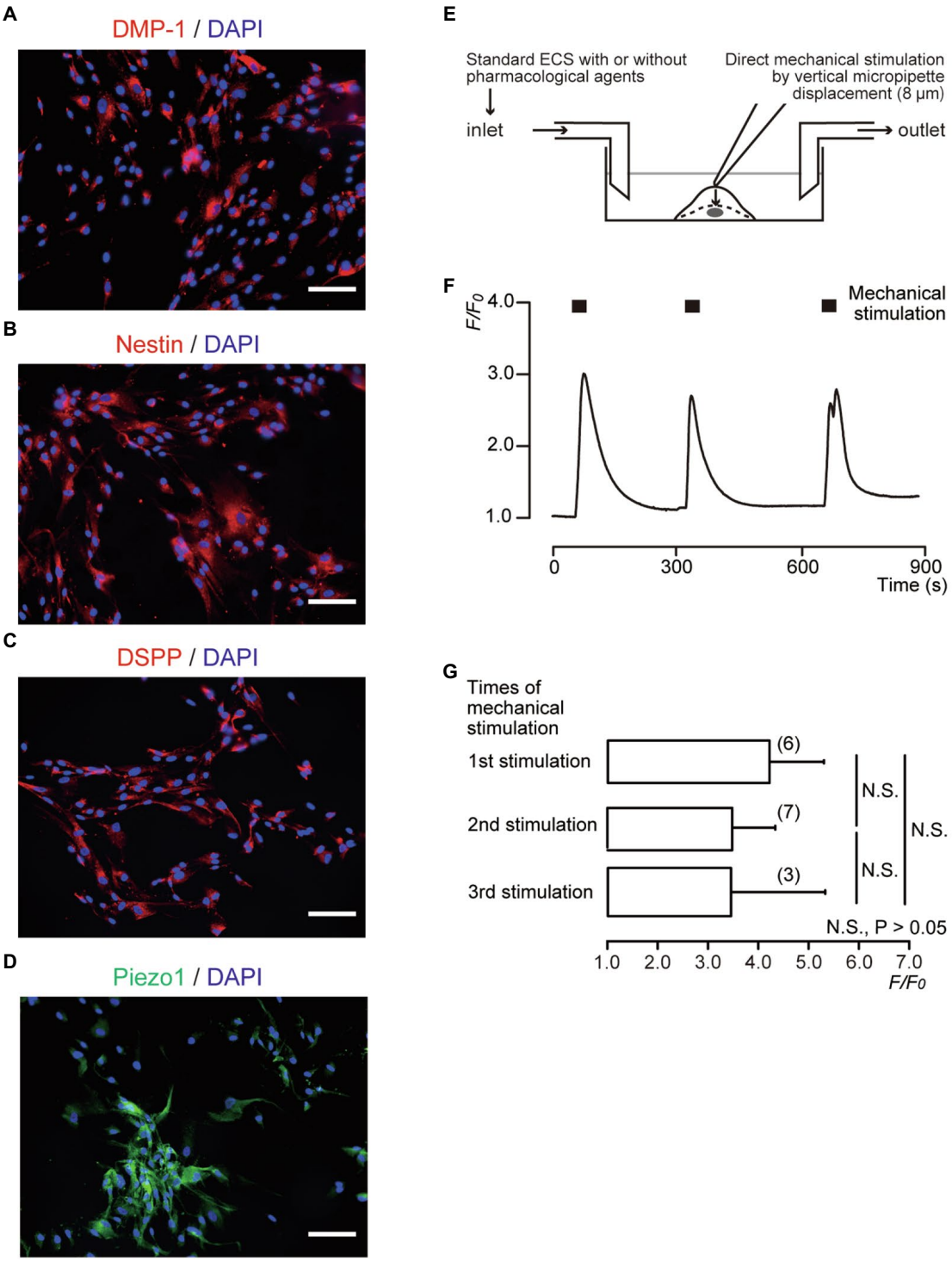


**FIGURE 1 |** Direct mechanical stimulation transiently increased $[Ca^{2+}]_i$ in dentin matrix protein 1 (DMP-1)-, nestin-, and dentin sialophosphoprotein (DSPP)-immunopositive human odontoblasts. **(A–D)** Human odontoblasts showed positive immunoreactivity to the DMP-1 (red in **A**), nestin (red in **B**), DSPP (red in **C**), and Piezo1 channels (green in **D**). Nuclei were represented in blue. Scale bar: 100 μm. No fluorescence was detected in the negative controls (not shown). **(E)** Experimental setup for the measurement of $Ca^{2+}$-sensitive dye fluorescence. Standard extracellular solution (standard ECS) with or without pharmacological Piezo1 channel activator/inhibitors was applied from inlet by a rapid gravity-fed perfusion system and aspirated using a vacuum pump. Diagram also shows mechanical stimulation induced by vertical micropipette displacement downward by 8.0 μm. **(F)** Representative trace of transient increases in $[Ca^{2+}]_i$ during repeated mechanical stimulations (black boxes). **(G)** Bar graph showing the $F/F_0$ values as a function of numbers of mechanical stimuli by vertical micropipette displacement (8 μm). Each bar indicates the mean ± SD. Numbers in parentheses indicate the number of experimented cells. N.S., not significant.

from capillary tubes using a DMZ Universal Puller (Zeitz Instruments, Martinsried, Germany). The micropipette was operated using a micromanipulator (UMp Micromanipulators; Sensapex, Oulu, Finland). The tip was positioned just above the target human odontoblast membrane, and the micropipette was moved vertically downward by 8.0 µm at a velocity of 2.0 µm/s (Sato et al., 2015; Shibukawa et al., 2015) to generate a focal mechanical stimulation (**Figure 1E**). Stimulation was applied for 22 s, after which the pipette was retracted at the same velocity. The stimulations were applied in series no more than three times to avoid unfavorable cell damage.

## Measurement of $Ca^{2+}$-Sensitive Dye Fluorescence

Human odontoblasts were incubated for 60 min at 37°C and 5% $CO_2$ in a standard solution containing 10 µM fura-2-acetoxymethyl ester (Dojindo Laboratories, Kumamoto, Japan) and 0.1% (*w*/*v*) pluronic acid F-127 (Life Technologies). They were then washed with a fresh standard solution. A dish containing fura-2-loaded human odontoblasts was mounted on the stage of a microscope (IX73; Olympus, Tokyo, Japan), which was installed with an HCImage system (Hamamatsu Photonic, Shizuoka, Japan), an excitation wavelength selector, and an intensified charge-coupled device camera system. Fura-2 fluorescence emission was recorded at 510 nm in response to alternating excitation wavelengths of 340 nm (F340) and 380 nm (F380). The intracellular free $Ca^{2+}$ concentration ($[Ca^{2+}]_i$) was defined as the fluorescence ratio ($R_{F340/F380}$) at two excitation wavelengths and then described as $F/F_0$ units; the $R_{F340/F380}$ value ($F$) was normalized to the resting value ($F_0$). All the experiments were performed at room temperature (28°C). Standard ECS with or without pharmacological Piezo1 channel activator/inhibitors was applied by superfusion using a rapid gravity-fed perfusion system (ValveLink8.2 Controller; AutoMate Scientific, Berkeley, CA, United States; **Figure 1E**).

## Measurement of Intercellular Distance

Human odontoblasts were imaged using an intensified charge-coupled device camera (Hamamatsu Photonic) and microscope (Olympus). The distance from a mechanically stimulated human odontoblast to each neighboring cell was determined from the images obtained (HCImage) by measuring the shortest distance between each pair of cells.

## Piezo1 Channel Knockdown by Gene Silencing With Short Hairpin RNA

To generate the odontoblasts transfected by shRNA, including vectors specific for human Piezo1 (shRNA-Piezo1 transfected cells) or an empty vector control (shRNA-Control transfected cells), the Lenti-X™ 293T cell line (Takara Bio Inc., Shiga, Japan) was used to produce lentiviral vector particles. Packaging plasmids pCAG-HIVgp (RIKEN BioResource Research Center, Tsukuba, Japan, RDB04394) and pCMV-VSV-G-RSV-Rev (RIKEN BioResource Research Center, RDB04393) were used for lentiviral vector packaging. Lentiviral vectors specific for human Piezo1 (Sigma-Aldrich) and a TRC2 empty vector control (Sigma-Aldrich) were used in this experiment. Viral supernatants were harvested after 72 h. Human odontoblasts with 60–80% confluency were transfected with lentiviral vector particles including shRNA and then incubated under normal growth conditions for 72 h.

## Immunostaining

Human odontoblasts were transferred to eight-well glass chambers (AGC Techno Glass Co., Ltd., Shizuoka, Japan) and maintained under culture conditions as described above. Cells were fixed with 4% paraformaldehyde (FUJIFILM Wako Pure Chemical Co., Osaka, Japan) and washed with 1× PBS (Thermo Fisher Scientific, Tokyo, Japan). After 10 min of incubation with blocking buffer (Nacalai Tesque, Kyoto, Japan) at room temperature, the following primary antibodies were applied for 6 h: mouse monoclonal anti-dentin matrix protein 1 (DMP-1; 1:200; sc-73,633, LFMb-31; Santa Cruz Biotechnology, Dallas, Texas, United States), mouse monoclonal anti-DSPP (1:200; sc-73,632, LFMb-21; Santa Cruz Biotechnology), or mouse monoclonal anti-nestin (1:200; sc-23927, 10c2; Santa Cruz Biotechnology). The secondary antibody (Alexa Fluor® 555 donkey anti-mouse; Thermo Fisher Scientific) was then applied for 1 h. Human odontoblasts, which were transfected with shRNA-Piezo1 and shRNA-Control, were also transferred to eight-well glass chambers (AGC Techno Glass Co., Ltd.), maintained in culture conditions, and fixed with 4% paraformaldehyde (FUJIFILM Wako Pure Chemical Co.). The cells were washed with 1× PBS (Thermo Fisher Scientific K.K.), and incubated for 10 min with blocking buffer (Nacalai Tesque) at room temperature. Next, Alexa Fluor® 488 conjugated rabbit polyclonal anti-Piezo1 (1:200; NBP1-78537 AF488; Novus Biologicals, LLC, Centennial, CO, United States) and Alexa Fluor® 594 conjugated rabbit polyclonal anti-Piezo2 (1:200; NBP1-78538 AF594; Novus Biologicals) were applied for 6 h. Stained samples were mounted in mounting medium with 4,6-diamidino-2-phenylindole (Abcam, Cambridge, United Kingdom). Immunostaining was observed and analyzed, and photographs were taken (as 8-bit TIFF images) using a fluorescence microscope (BZ-X710; Keyence, Osaka, Japan). For the negative control, the cells were incubated with non-immune antibodies diluted to equivalent concentrations to those of the primary antibodies (data not shown). For shRNA-Piezo1 transfected and shRNA-Control transfected cells, TIFF images obtained with 8-bit of 1,920 × 1,440 pixels were converted to reversed grayscale. Then, the percentage area of the Piezo1- or Piezo2-immunopositive cells was measured using automated thresholds of ImageJ software (NIH, Bethesda, MD, United States).

## Mineralization Assay

Human odontoblasts were grown to full confluency in basal medium, and then transferred to mineralization medium (10 mM β-glycerophosphate and 100 µg/ml ascorbic acid in basal medium) for growth at 37°C in 5% $CO_2$. To determine the effects of Piezo1 activity on mineralization, the cells were cultured in mineralization medium without (as control)

or with the pharmacological Piezo1 modifier, Yoda1 (2 μM), Dooku1 (10 μM), or Yoda1 (2 μM) and Dooku1 (10 μM) for 28 days. The odontoblasts transfected with shRNA, including vectors specific for human Piezo1, or including an empty vector control (see above), were also grown to full confluency in basal medium, and then transferred to mineralization medium at 37°C in 5% $CO_2$ for 28 days. During the 28-day culture period, mineralization media with or without pharmacological agents were changed twice a week (Kimura et al., 2016). To detect calcium deposition, the cells were subjected to Alizarin red staining, and the mineralizing efficiencies were measured using ImageJ software (NIH). Images were obtained with a digital camera (Sony, Tokyo, Japan), converted to 32-bit, and converted into reversed grayscale. Regions of interest (ROIs) were then determined for each whole well to measure the mean luminance intensities of the total pixel numbers (I) of the ROI. Mineralizing efficiencies were normalized and represented as $I/I_0$ units, and the intensities ($I$) of Alizarin red staining were normalized to the mean intensity values of areas without cells ($I_0$).

### Statistical Analysis

Data are expressed as the mean ± SE or SD of the mean of $N$ observations, where $N$ represents the number of experiments or cells tested. The Kruskal-Wallis test, Friedman test, and Dunn's *post-hoc* test were used to determine non-parametric statistical significance. Parametric statistical significance was determined using a two-tailed Student's $t$-test to analyze the percentage areas of Piezo1/2 channel-immunopositive cells in the immunofluorescence analyses. Statistical significance was set at $p < 0.05$. Statistical analysis was performed using GraphPad Prism 5.0 (GraphPad Software, La Jolla, CA, United States).

## RESULTS

### Direct Mechanical Stimulation to Human Odontoblasts Transiently Increased $[Ca^{2+}]_i$

We observed distinct DMP-1, nestin, and DSPP immunoreactivity in human odontoblasts (**Figures 1A–C**). In addition, odontoblasts also expressed Piezo1 immunoreactivity (**Figure 1D**). Cells expressing odontoblast marker proteins were loaded with fura-2, and $[Ca^{2+}]_i$ was measured. When we applied mechanical stimulations to single human odontoblasts using a glass micropipette moving vertically (8 μm) in a downward direction from a position just above the surface (0 μm; **Figure 1E**), in the presence of extracellular $Ca^{2+}$, $[Ca^{2+}]_i$ was increased to a peak value of 4.20 ± 1.08 $F/F_0$ units for first stimulation ($N = 6$; **Figure 1F**). After $[Ca^{2+}]_i$ returned to near-resting levels, further application of mechanical stimulation transiently increased $[Ca^{2+}]_i$ in human odontoblasts. Repeated mechanical stimulation did not show any desensitizing effect on the $[Ca^{2+}]_i$ increases after the third application ($p > 0.05$; **Figures 1F,G**).

### Direct Mechanical Stimulation to Human Odontoblasts Transiently Increased $[Ca^{2+}]_i$ in Stimulated Human Odontoblasts and Neighboring Cells to the Stimulated Cells

In the presence of extracellular $Ca^{2+}$, during the application of focal and direct mechanical stimulation to single human odontoblasts (8.0 μm in-depth), we observed transient increases in $[Ca^{2+}]_i$ in the mechanically stimulated human odontoblasts (black line, **Figure 2A**) to a peak value of 4.21 ± 1.46 $F/F_0$ units ($N = 38$; black circle, **Figure 2B**). In addition, we observed transient increases in $[Ca^{2+}]_i$ in the neighboring human odontoblasts (red lines, **Figure 2A**) during mechanical stimulation. Note that these cells were not in physical contact with each other. The plots in **Figure 2B** show $F/F_0$ values as a function of the distance from the stimulated odontoblast (black circle) to neighboring odontoblasts (red circles). The peak values of $[Ca^{2+}]_i$ were 2.52 ± 1.45 ($N = 9$), 1.59 ± 0.55 ($N = 15$), 1.34 ± 0.32 ($N = 8$), 1.07 ± 0.03 ($N = 4$), 1.11 ± 0.09 ($N = 6$), 1.06 ± 0.03 ($N = 6$), and 1.02 ± 0.01 ($N = 5$) $F/F_0$ units in human odontoblasts located within distances of 0–10 μm, 11–20 μm, 21–30 μm, 31–40 μm, 41–50 μm, 51–60 μm, and 61–70 μm from mechanically stimulated human odontoblasts, respectively (red circles, **Figure 2B**). The amplitude of the $[Ca^{2+}]_i$ increases in neighboring human odontoblasts was reduced by increasing their distance from mechanically stimulated human odontoblasts. The kinetics of the distance-dependent attenuation of $[Ca^{2+}]_i$ were described well by a single exponential function (dotted line, **Figure 2B**). The spatial constants of the distance-dependent decrease in $[Ca^{2+}]_i$ were 6.11 ± 0.76 μm for neighboring odontoblasts. In addition, we observed a delay in the increase in $[Ca^{2+}]_i$ in the nearby odontoblasts during the mechanical stimulation of single odontoblasts (time when the mechanical stimulation applied to the stimulated odontoblasts was set to 0 s; vertical dotted line, **Figure 2A**). The time delay increased with an increase in the distance from the mechanically stimulated odontoblasts (**Figure 2C**). The significant time delay in the increase in $[Ca^{2+}]_i$ in the neighboring odontoblasts located 51–60 μm and 61–70 μm away from mechanically stimulated odontoblasts was observed compared to that in the cells located at 0–10 μm (**Figure 2C**). The time delay was ranged from 0.95 ± 0.47 s at 0–10 μm away to 3.03 ± 1.04 s at 61–70 μm away from mechanically stimulated cells.

### $[Ca^{2+}]_i$ Is Increased by a Selective Pharmacological Piezo1 Channel Activator

To pharmacologically activate Piezo1 channels in human odontoblasts, Yoda1 was used as a selective Piezo1 channel activator. In the presence of external $Ca^{2+}$ (2.5 mM), the application of 2 μM Yoda1 to human odontoblasts showed a rapid and transient $[Ca^{2+}]_i$ increase (**Figures 3A,C**), reaching a peak value of 2.38 ± 0.58 ($N = 6$; **Figure 3B**), and 2.36 ± 0.43 ($N = 12$) in $F/F_0$ units (**Figure 3D**), followed by a rapid decay to near baseline levels ($F/F_0 = 1$). Yoda1 induced-$[Ca^{2+}]_i$ increases were significantly and reversibly inhibited by extracellular 1 μM $Gd^{3+}$, a non-selective Piezo1 channel inhibitor to 1.36 ± 0.17 ($N = 6$; **Figures 3A,B**) and 10 μM Dooku1, and a pharmacological

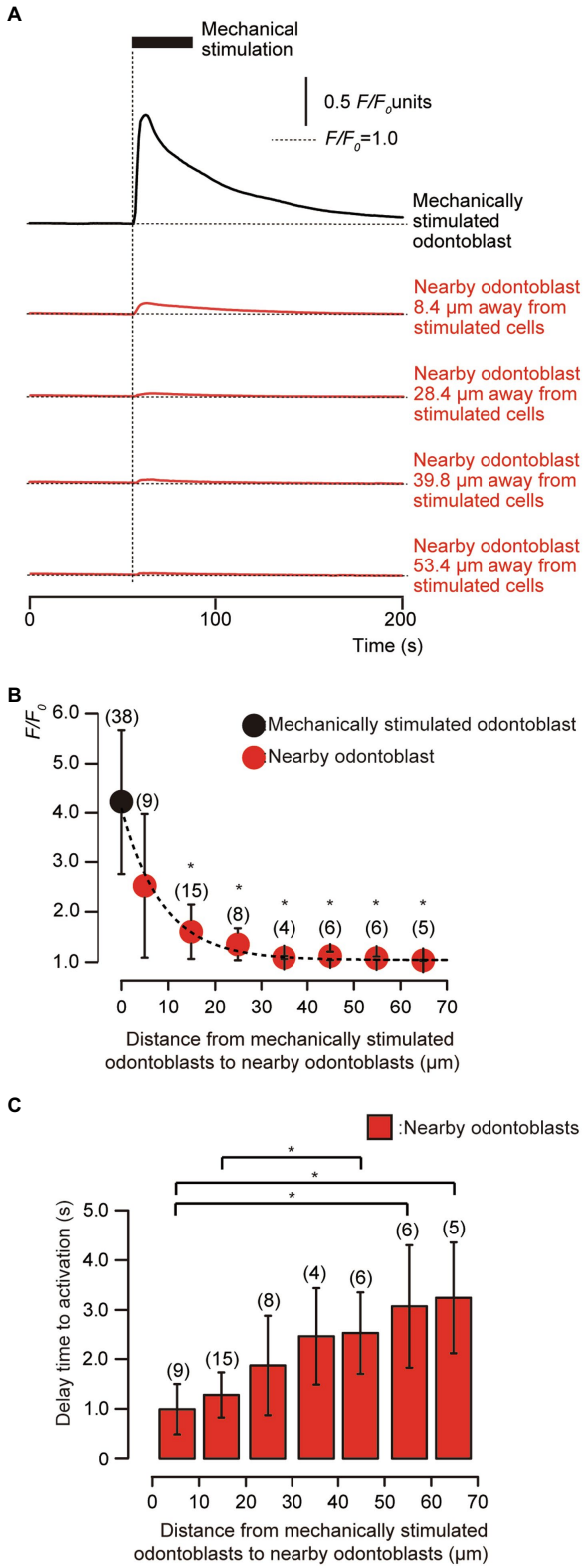


**FIGURE 2 |** Transient $[Ca^{2+}]_i$ increases in mechanical-stimulated human odontoblast and neighboring human odontoblasts to the stimulated cells. **(A)** Representative traces indicating transiently increased $[Ca^{2+}]_i$ from a mechanically stimulated human odontoblast (black line) and neighboring human odontoblasts (red lines) in standard extracellular solution. Horizontal dotted lines indicate the baseline ($F/F_0 = 1.0$) for each response, while vertical dotted line represents the time when mechanical stimulation was applied. The black box at the top shows the timing of mechanical stimulation by the displacement of a micropipette to a depth of 8.0 μm. Responses from the nearby human odontoblasts were recorded in cells at 8.4 μm, 28.4 μm, 39.8 μm, and 53.4 μm away from the stimulated human odontoblast. **(B)** The $F/F_0$ values of the mechanically stimulated odontoblasts (black circle) and nearby odontoblasts (red circles) located within 0–10 μm, 11–20 μm, 21–30 μm, 31–40 μm, 41–50 μm, 51–60 μm, and 61–70 μm from the stimulated human odontoblasts are shown. The kinetics of the distance-dependent decrease of $[Ca^{2+}]_i$ were described well by the single exponential function (dotted line), showing spatial constants of the distance-dependent decrease of 6.11 ± 0.76 μm. Circles indicate the mean ± SD. Numbers in parentheses indicate the number of cells tested. The $[Ca^{2+}]_i$ increases in neighboring odontoblasts were reduced by increasing their distance from mechanically stimulated cells. **(C)** Bar graph representing the mean time to increases in $[Ca^{2+}]_i$ in neighboring odontoblasts, during the mechanical stimulation to single odontoblasts. The delay time in $[Ca^{2+}]_i$ increase was measured by calculating the time between the onset of the mechanical stimulation of the odontoblasts and time require to achieve the rising phase for each $[Ca^{2+}]_i$ response in neighboring cells. Each data point indicates the mean ± SD from the number of cells tested (numbers in parentheses). Statistically significant differences in **(B,C)** between values are indicated by asterisks. *$p < 0.05$.

and selective Piezo1 channel inhibitor to 1.33 ± 0.18 ($N = 12$) in $F/F_0$ units, reversibly (**Figures 3C,D**).

## Pharmacological Piezo1 Channel Inhibitors Suppressed Direct Mechanical Stimulation-Induced $[Ca^{2+}]_i$ Increases in Human Odontoblasts

We examined the effects of 1 μM $Gd^{3+}$ (**Figures 4A,B**) and 10 μM Dooku1 (**Figures 4C,D**) on the direct mechanical stimulation-induced $[Ca^{2+}]_i$ increase in single human odontoblasts. The $[Ca^{2+}]_i$ increases induced by mechanical stimulation [3.81 ± 0.84 in $F/F_0$ units ($N = 4$) in **Figures 4A,B** and 3.16 ± 0.59 in $F/F_0$ units ($N = 6$) in **Figures 4C,D** as the control, respectively] were reversibly and significantly inhibited by the application of 1 μM $Gd^{3+}$ to 1.47 ± 0.31 ($N = 4$; **Figures 4A,B**) and 10 μM Dooku1 to 1.15 ± 0.15 ($N = 6$) in $F/F_0$ units (**Figures 4C,D**). The $[Ca^{2+}]_i$ induced by mechanical stimulation was recovered to 2.38 ± 0.43 ($N = 4$) after $Gd^{3+}$ and to 1.81 ± 0.41 ($N = 6$) after Dooku1 application (**Figure 4**).

## Piezo1 Channel Knockdown by Short Hairpin RNA Reduced the Functional Expression of Piezo1 but Not Piezo2 Channels

We further investigated mechanical stimulation-induced $[Ca^{2+}]_i$ increases in human odontoblasts transfected with shRNA with a vector specific for human Piezo1, and an empty vector control. In the immunofluorescence analysis, we observed immunoreactivity not only of the Piezo1 channels (green, **Figures 5A,E**), but also of the Piezo2 channels (red, **Figures 5B,E**) in the cells transfected with an empty vector control. In the cells transfected by shRNA with a vector specific for human Piezo1 (shRNA-Piezo1 transfected cells), we observed a significant

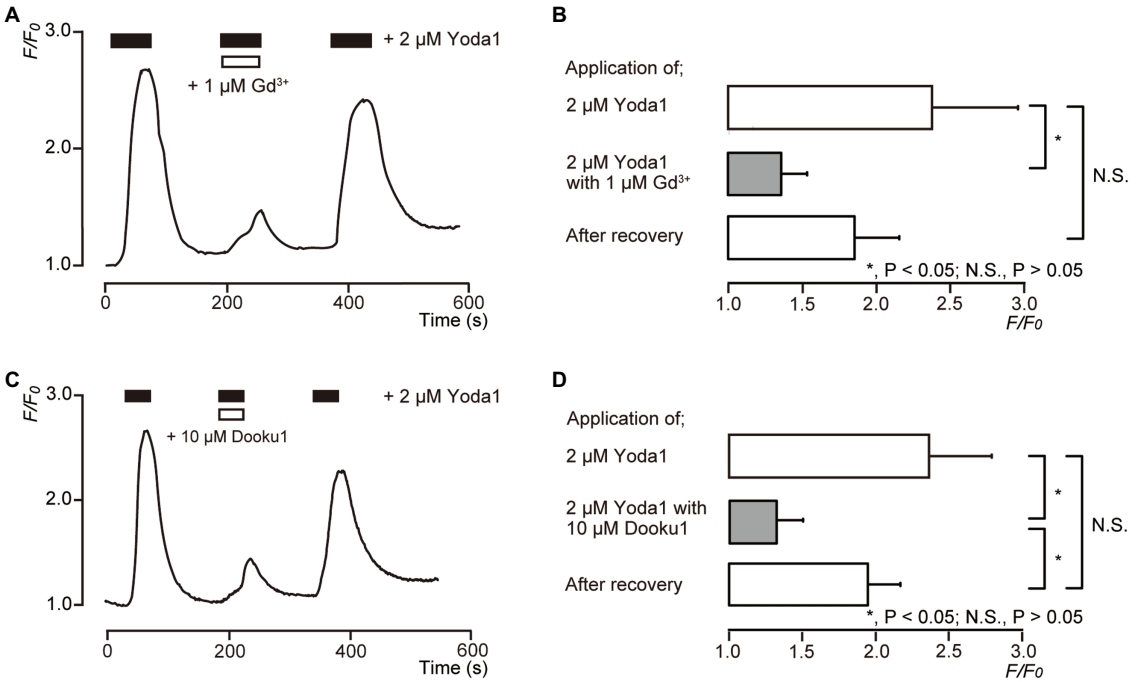


**FIGURE 3 |** Piezo1 channel activator induces $[Ca^{2+}]_i$ increases in human odontoblasts. **(A,C)** Representative traces of transient $[Ca^{2+}]_i$ increase in response to 2 μM Yoda1 in standard extracellular solution are shown. Addition of 1 μM $Gd^{3+}$ **(A)** or 10 μM Dooku1 **(C)** inhibited Yoda1-induced $[Ca^{2+}]_i$ increases. In each figure, the boxes indicate the timings when the test solution, including pharmacological activator (black boxes at the top) or inhibitors (white boxes at the top), were applied. **(B,D)** Bar graphs representing values of $F/F_0$ for the increases in $[Ca^{2+}]_i$ by 2 μM Yoda1 with (gray columns) or without (open columns) 1 μM $Gd^{3+}$ **(B)** or 10 μM Dooku1 **(D)**. The pharmacological activators and inhibitors used are indicated on the left side of the graphs. The resting value is defined as $F/F_0 = 1.0$. Each bar indicates the mean ± SE of six **(B)** and 12 **(D)** experiments. Asterisks denote statistically significant differences between columns (shown by solid lines): $^*p < 0.05$.

reduction in the percentage area of Piezo1-immunopositive cells (3.14 ± 0.71%; $N = 5$; **Figures 5C**,**E**) compared to that in the cells transfected by shRNA with an empty vector control (as shRNA-Control transfected cells; 11.5 ± 4.25%; $N = 5$; **Figures 5A**,**E**). However, we did not observe any significant changes in the area of Piezo2-immunopositive cells in both cells: 6.38 ± 2.44% ($N = 5$, **Figures 5B**,**E**) in the shRNA-Control transfected cells and 6.29 ± 2.49% ($N = 5$, **Figures 5D**,**E**) in the shRNA-Piezo1 transfected cells. In addition, in the presence of extracellular $Ca^{2+}$, we observed significant changes in $F/F_0$ units by mechanical stimulation-induced $[Ca^{2+}]_i$ increases in cells between the shRNA-Piezo1 transfected (1.34 ± 0.29; $N = 7$) and shRNA-Control transfected cells (4.74 ± 1.25; $N = 6$; **Figures 5F**,**G**).

## Activation of Piezo1 Channel by the Pharmacological Modifiers Reduced Mineralization

We investigated the effects of Piezo1 channel activity on mineralization induced by human odontoblasts. Alizarin red staining (**Figure 6A**) was determined to be indicative of the mineralization levels based on the staining intensity (see **Materials and Methods**) represented as $I/I_0$ units; the intensities ($I$) of the stains were normalized to the mean intensities of adjacent areas without cells ($I_0$; **Figure 6B**). The application of 2 μM Yoda1, or 2 μM Yoda1 and 10 μM Dooku1, significantly reduced their mineralization levels compared to the level without these pharmacological Piezo1 channel modifiers. In addition, the level in the presence of 2 μM Yoda1 was significantly lower than that in the presence of 10 μM Dooku1.

## Piezo1 Channel Knockdown by shRNA Enhanced Mineralization

We also examined the contribution of Piezo1 channel activity to mineralization efficiency. The mineralization level represented by Alizarin red staining (**Figure 7A**) in the shRNA-Piezo1 transfected cells was significantly higher than that in the shRNA-Control transfected cells (**Figure 7B**).

# DISCUSSION

The results showed that human odontoblasts, which showed DMP-1-, nestin-, and DSPP-immunoreactivity, functionally express Piezo1 channels activated by Yoda1 pharmacologically and by direct mechanical stimulation. Both Yoda1 induced- and direct mechanical stimulation-induced-$[Ca^{2+}]_i$ increases were sensitive to extracellular $Gd^{3+}$ and Dooku1, which are pharmacological non-selective and selective Piezo1 channel inhibitors, respectively. In human odontoblasts, mechanical stimulation-induced-$[Ca^{2+}]_i$ increases also mediated intercellular signal networks among odontoblasts, as previously reported

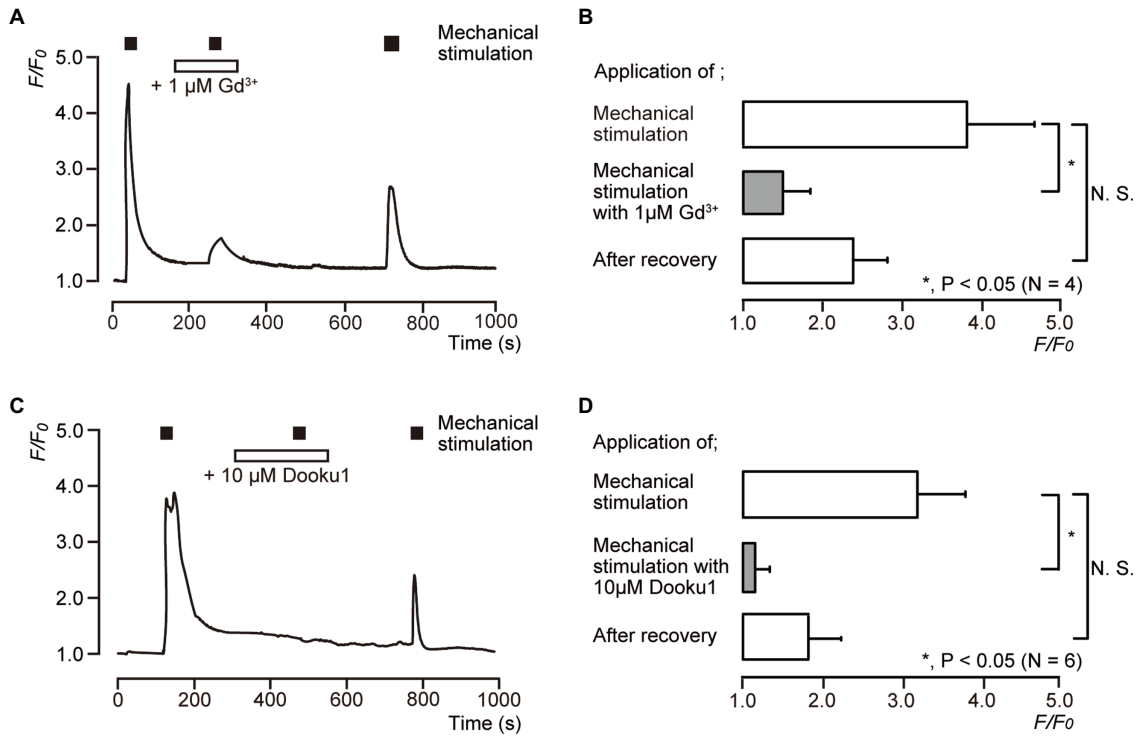


**FIGURE 4 |** Direct mechanical stimulation-evoked $[Ca^{2+}]_i$ increases mediated by a Piezo1 channel. **(A,C)** Representative traces of transient increases in $[Ca^{2+}]_i$ during mechanical stimulations induced by vertical micropipette displacement downward by 8.0 μm (black boxes at the top in **A,C**) in standard extracellular solution with (white boxes at the top) or without 1 μM $Gd^{3+}$ **(A)** or 10 μM Dooku1 **(C)**. **(B,D)** Bar graphs of the values of $[Ca^{2+}]_i$ increases induced by mechanical stimulation (to 8.0 μm) without (open columns) or with (gray columns) pharmacological inhibitors, 1 μM $Gd^{3+}$ **(B)**, or 10 μM Dooku1 **(D)**. Each of the most lower open columns indicates the $F/F_0$ values after recovery. The resting value is shown as $F/F_0 = 1.0$. Each bar indicates the mean ± SD of four **(B)** and six **(D)** cells tested. Asterisks denote statistically significant differences between columns (shown by solid lines): $^*p < 0.05$; N.S., not significant.

in rat studies (Sato et al., 2015; Shibukawa et al., 2015). These mechanical stimulation-induced $[Ca^{2+}]_i$ responses were almost completely abolished in cells when Piezo1 channels were knocked down by shRNA. In addition, Alizarin red staining indicated that pharmacological Piezo1 channel activation by Yoda1 significantly suppressed mineralization, and the shRNA-mediated knockdown of Piezo1 significantly enhanced mineralization.

We previously found that odontoblasts can detect mechanical stimuli as cellular deformation originating from dentinal fluid movement by dentin stimuli and act as sensory receptor cells to generate dentinal sensitivity. The mechanism underlying the generation of dentinal sensitivity has been termed the odontoblast hydrodynamic receptor model (Shibukawa et al., 2015). The stimuli to the dentin surface transformed into dentinal fluid movements and induced cell membrane deformation in odontoblasts. Cell deformation activates mechanosensitive transient receptor potential (TRP) channels, such as TRP vanilloid subfamily member 1 (TRPV1), TRPV2, TRPV4, and TRP ankyrin 1 (TRPA1) channels, increasing $[Ca^{2+}]_i$ through $Ca^{2+}$ influx (Tsumura et al., 2012, 2013; Sato et al., 2013, 2018; Shibukawa et al., 2015). The $[Ca^{2+}]_i$ increase established intercellular odontoblast-odontoblast and odontoblast-neuron signal communication mediated by extracellular signaling molecules, ATP, and glutamate, which are released from mechanically stimulated odontoblasts (Sato et al., 2015; Shibukawa et al., 2015; Nishiyama et al., 2016). The released ATP (from pannexin-1 channels in odontoblasts triggered by the $[Ca^{2+}]_i$ increase) activates ionotropic ATP receptor subtype 3 ($P2X_3$ receptors) in the intradental Aδ neurons. The activation of $P2X_3$ receptors induces an action potential in pulpal Aδ neurons, indicative of the generation of dentinal sensitivity (Sato et al., 2018). Additionally, in line with the present results, the application of selective Piezo1 channel inhibitors, GsMTx4, also inhibited synaptic-like responses in TG neurons evoked by the direct mechanical stimulation of odontoblasts. Together with the present and previous results, Piezo1 channels in odontoblasts are involved in detecting cell membrane deformation due to dentinal fluid movements by the stimuli applied to the dentin surface to generate dentinal sensitivity, and in mediating inter-odontoblast signal networks. Indeed, the inhibition of Piezo1 channels by the systemic administration of GsMTx4 and the somatic elimination of odontoblasts in the dentin-pulp border (using Cre/LoxP-based technology; Zhao et al., 2021) almost completely abolished nociceptive behaviors by cold stimuli to the exposed dentin surface in rats/transgenic mice showing dentinal sensitivity (personal communication from YS).

In line with our results, it has been described that Piezo1 channels are expressed not only in multipotent stem cells from

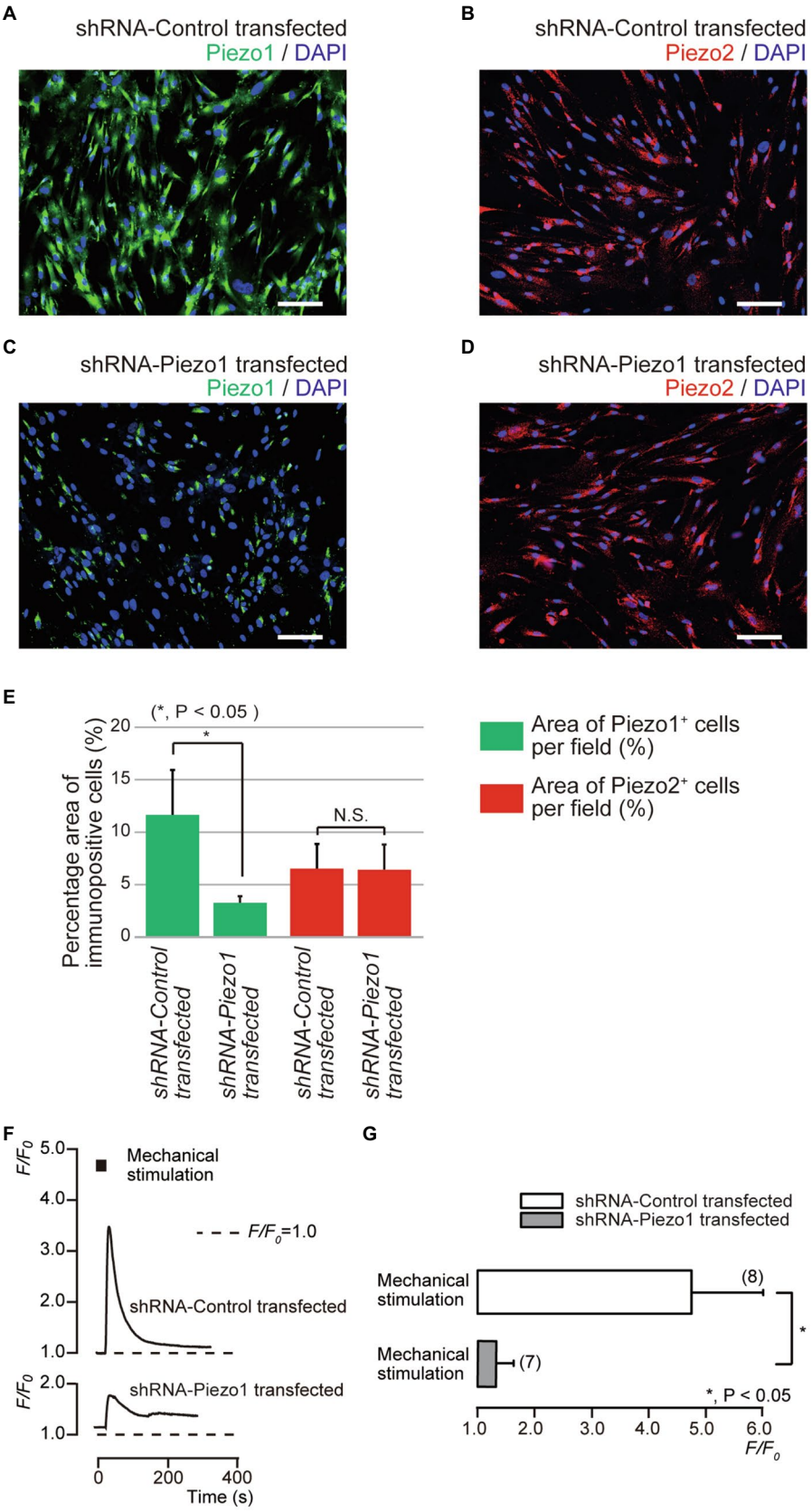
A
shRNA-Control transfected
Piezo1 / DAPI
B
shRNA-Control transfected
Piezo2 / DAPI
C
shRNA-Piezo1 transfected
Piezo1 / DAPI
D
shRNA-Piezo1 transfected
Piezo2 / DAPI
E
(*, P < 0.05 )
Percentage area of immunopositive cells (%)
20
15
10
5
0
*
N.S.
shRNA-Control transfected
shRNA-Piezo1 transfected
shRNA-Control transfected
shRNA-Piezo1 transfected
Area of Piezo1+ cells per field (%)
Area of Piezo2+ cells per field (%)
F
F/F0
5.0
4.0
3.0
2.0
1.0
Mechanical stimulation
F/F0=1.0
shRNA-Control transfected
F/F0
2.0
1.0
shRNA-Piezo1 transfected
0
200
400
Time (s)
G
shRNA-Control transfected
shRNA-Piezo1 transfected
Mechanical stimulation
(8)
Mechanical stimulation
(7)
*
*, P < 0.05
1.0
2.0
3.0
4.0
5.0
6.0
F/F0

*(Continued)*

**FIGURE 5 |** Piezo1 channel knockdown by gene silencing with short hairpin RNA (shRNA) reduced the functional expression of Piezo1 not Piezo2 channels. **(A–D)** Immunoreactivity to the Piezo1 channels (green in **A,C**) or the Piezo2 channels (red in **B,D**) in human odontoblasts transfected by shRNA including a vector specific for human Piezo1 **(C,D)**, or including an empty vector control **(A,B)**. Nuclei are shown in blue. Scale bar: 100 μm. No fluorescence was detected in the negative controls (not shown). **(E)** Bar graph showing the percentage area of the Piezo1 channel-immunopositive cells (%; green columns), and those of Piezo2 channel-immunopositive cells (%; red columns) in immunofluorescence analysis from human odontoblasts transfected by shRNA including a vector specific for human Piezo1 (second left and most right columns), or including an empty vector control (most left and third left). Each bar indicates the mean ± SD of five experiments. **(F)** Representative traces of transient increases in $[Ca^{2+}]_i$ during mechanical stimulations induced by vertical micropipette displacement downward by 8.0 μm (black boxes at the top) in standard extracellular solution in cells transfected by shRNA including a vector specific for human Piezo1 (shRNA-Piezo1 transfected), or including an empty vector control (shRNA-Control transfected). **(G)** Bar graph of the values of $[Ca^{2+}]_i$ increases induced by mechanical stimulation (8.0 μm) in cells transfected by shRNA including a vector specific for human Piezo1 (gray column), or including an empty vector control (open column). The resting value is shown as $F/F_0 = 1.0$. The numbers in parentheses indicate the number of cells tested. Asterisks denote statistically significant differences between columns (shown by solid line in G): $^*p < 0.05$; N.S., not significant.

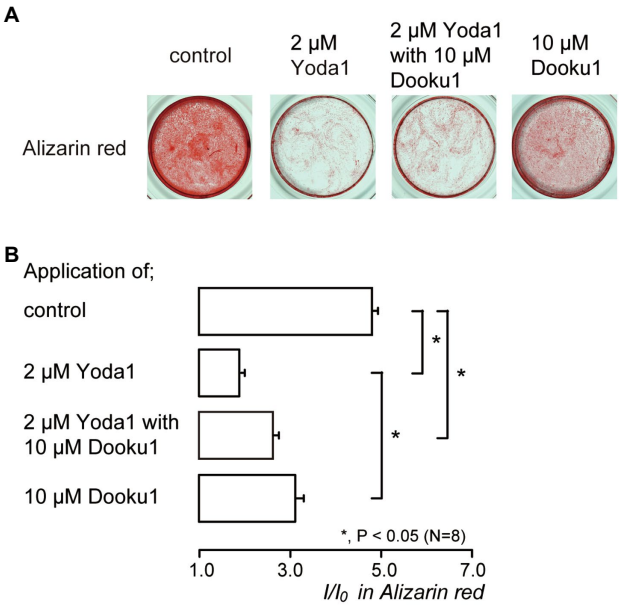


**FIGURE 6 |** Piezo1 channel activation decreases the mineralization levels. **(A)** Human odontoblasts were cultured for 28 days in mineralization medium with 2 μM Yoda1 (second left), 2 μM Yoda1 and 10 μM Dooku1 (third left), 10 μM Dooku1 (right most), or without these channel modifiers (left most) at pH 7.4, and stained by Alizarin red (red, calcium deposition). **(B)** Mineralization levels without (control; upper most column) or with 2 μM Yoda1 (second column), 2 μM Yoda1 and 10 μM Dooku1 (third column), and 10 μM Dooku1 (lower column), assessed by Alizarin red staining. The mineralization levels were 4.80 ± 0.13 $I/I_0$ in the absence of Piezo1 channel modifiers (as controls), while those 1.96 ± 0.04 $I/I_0$ with 2 μM Yoda1, 2.63 ± 0.12 $I/I_0$ with 2 μM Yoda1 and 10 μM Dooku1, and 3.11 ± 0.18 $I/I_0$ with 10 μM Dooku1. Each column denotes the mean ± SE from eight experiments. Statistically significant differences between columns (shown by solid lines) are indicated by asterisks. $^*p < 0.05$.

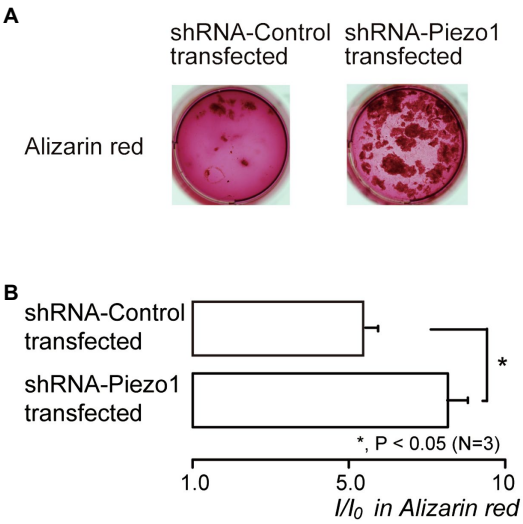


**FIGURE 7 |** Piezo1 channel knockdown by shRNA enhances the mineralization levels. **(A)** Human odontoblasts transfected by shRNA including a vector specific for human Piezo1 (right; shRNA-Piezo1 transfected) or including an empty vector control (left; shRNA-Control transfected) were cultured for 28 days in mineralization medium, and subjected to the Alizarin red staining (red indicative of calcium deposition). **(B)** The mineralization levels in the cells of shRNA-Control transfected (upper column) and shRNA-Piezo1 transfected (lower column), assessed by Alizarin red staining. The mineralization levels were 5.95 ± 0.36 $I/I_0$ in the shRNA-Control transfected cells, and 8.30 ± 0.59 $I/I_0$ in the shRNA-Piezo1 transfected cells. Each column indicates the mean ± SE from three experiments. Statistically significant differences between columns (solid line) are indicated by asterisks. $^*p < 0.05$.

human exfoliated deciduous teeth (SHED), but also in odontoblast processes (Miyazaki et al., 2019). In addition to the mechanosensory transduction roles of odontoblasts, Piezo1 channels also mediate hydrostatic pressure-induced differentiation of odontoblasts from SHED (Miyazaki et al., 2019). In the Alizarin red staining of the present study, however, the pharmacological activation of the Piezo1 channel significantly suppressed mineralization efficiency. In addition, the intensity of Alizarin red staining of shRNA-Piezo1 transfected cells was significantly higher than that in shRNA-Control transfected cells. These results indicate that Piezo1 channels in odontoblasts may negatively regulate not only reactionary dentinogenesis induced by cell membrane deformation due to dentinal fluid movements by the stimuli applied to the exposed dentin surface, but also physiological/developmental dentinogenesis. In contrast, the activation of mechanosensitive- and high-pH sensitive-TRPA1 channels in odontoblasts positively modulates mineralization in physiological, developmental, and pathological conditions [e.g., $Ca(OH)_2$ or mineral trioxide aggregate (MTA) application on dentin; Kimura et al., 2016]. Although further studies are needed, these convergent results suggest that, among odontoblast-expressing mechanosensitive cation channels, including TRPV1, TRPV2, TRPV4, TRPA1, and Piezo1 channels, their functional roles in sensory transduction and dentin formation are different.

Recent evidence have indicated that mouse odontoblasts also express Piezo2 channels (Khatibi Shahidi et al., 2015; Krivanek et al., 2020). In line with these results, we successfully observed Piezo2-immunoreactivity in both shRNA-Piezo1 transfected and shRNA-Control transfected cells. Thus, we could not exclude the possibility that Piezo2 channels are also involved in mechanosensory transduction in odontoblasts. However, further study will be needed to examine how Piezo2 channels contribute to the sensory transduction sequences, and what differences exist between the roles of Piezo1 and Piezo2 channels in cellular function. In addition, in endothelial cells, it has been demonstrated that Piezo1 channels regulate TRPV4 channel openings. In the present study, the pharmacological Piezo1 inhibitors $Gd^{3+}$ (1 μM) and Dooku1 (10 μM) almost completely suppressed direct mechanical stimulation-induced $[Ca^{2+}]_i$ increases in single human odontoblasts. We also only observed small residual responses in mechanical stimulation-induced $[Ca^{2+}]_i$ increases in shRNA-Piezo1 transfected cells compared to those in the shRNA-Control transfected cells. Therefore, together with the present results, Piezo1 channels may act upstream of mechanosensitive cation channels, including TRPV1, TRPV2, TRPV4, and TRPA1 channels, as well as Piezo2 channels, in odontoblasts.

In conclusion, we demonstrated that human odontoblasts functionally express Piezo1 channels, and mechanical stimulation-induced-$[Ca^{2+}]_i$ increases mediate the intercellular signaling networks among them. Piezo1 channels predominantly contribute to the detection of cellular deformation, such as mechanical stimulation, induced by dentinal fluid movements in dentinal tubules, during various stimuli applied to the exposed human dentin surface, such as enamel lesions including dental caries and/or acid erosion. However, Piezo1 channel activity negatively regulates not only reactionary dentinogenesis, but also physiological/developmental dentinogenesis. This suggests that Piezo1 channel activity may physiologically prevent the lifelong loss of volume in the pulp chamber by excessive dentin formation induced by mechanical stimuli applied on the teeth, such as mastication.

## DATA AVAILABILITY STATEMENT

The original contributions presented in the study are included in the article/supplementary material; further inquiries can be directed to the corresponding author.

## AUTHOR CONTRIBUTIONS

MM, MK, TI, and YS conceived and designed the experiments. MM, MK, TO, TN, SO, MA, SN, and TA performed the experiments. MM, MK, TO, TN, SO, MA, SN, TA, TI, and YS were responsible for analyzing and interpreting the data and drafting and critically revising the intellectual content of the article. TI and YS were responsible for the final approval of the version to be submitted or published. All authors contributed to the article and approved the submitted version.

## FUNDING

This work was supported by grants-in-aid (no. 19K10117/19H03833) for Scientific Research from MEXT of Japan and the Private University Research Branding Project from MEXT of Japan [Multidisciplinary Research Center for Jaw Disease (MRCJD): Achieving Longevity and Sustainability by Comprehensive Reconstruction of Oral and Maxillofacial functions].

## REFERENCES

Bagriantsev, S. N., Gracheva, E. O., and Gallagher, P. G. (2014). Piezo proteins: regulators of mechanosensation and other cellular processes. *J. Biol. Chem.* 289, 31673–31681. doi: 10.1074/jbc.R114.612697

Beech, D. J., and Xiao, B. (2018). Piezo channel mechanisms in health and disease. *J. Physiol.* 596:965. doi: 10.1113/JP274395

Borbiro, I., and Rohacs, T. (2017). Regulation of Piezo channels by cellular signaling pathways. *Curr. Top. Membr.* 79, 245–261. doi: 10.1016/bs.ctm.2016.10.002

Chesler, A. T., Szczot, M., Bharucha-Goebel, D., Čeko, M., Donkervoort, S., Laubacher, C., et al. (2016). The role of PIEZO2 in human mechanosensation. *N. Engl. J. Med.* 375, 1355–1364. doi: 10.1056/NEJMoa1602812

Coste, B., Mathur, J., Schmidt, M., Earley, T. J., Ranade, S., Petrus, M. J., et al. (2010). Piezo1 and Piezo2 are essential components of distinct mechanically activated cation channels. *Science* 330, 55–60. doi: 10.1126/science.1193270

Dalghi, M. G., Clayton, D. R., Ruiz, W. G., Al-Bataineh, M. M., Satlin, L. M., Kleyman, T. R., et al. (2019). Expression and distribution of PIEZO1 in the mouse urinary tract. *Am. J. Physiol. Ren. Physiol.* 317, F303–F321. doi: 10.1152/ajprenal.00214.2019

Ermakov, Y. A., Kamaraju, K., Sengupta, K., and Sukharev, S. (2010). Gadolinium ions block mechanosensitive channels by altering the packing and lateral pressure of anionic lipids. *Biophys. J.* 98, 1018–1027. doi: 10.1016/j.bpj.2009.11.044

Evans, E. L., Cuthbertson, K., Endesh, N., Rode, B., Blythe, N. M., Hyman, A. J., et al. (2018). Yoda1 analogue (Dooku1) which antagonizes Yoda1-evoked activation of Piezo1 and aortic relaxation. *Br. J. Pharmacol.* 175, 1744–1759. doi: 10.1111/bph.14188

Ichikawa, H., Kim, H.-J., Shuprisha, A., Shikano, T., Tsumura, M., Shibukawa, Y., et al. (2012). Voltage-dependent sodium channels and calcium-activated potassium channels in human odontoblasts in vitro. *J. Endod.* 38, 1355–1362. doi: 10.1016/j.joen.2012.06.015

Khatibi Shahidi, M., Krivanek, J., Kaukua, N., Ernfors, P., Hladik, L., Kostal, V., et al. (2015). Three-dimensional imaging reveals new compartments and structural adaptations in odontoblasts. *J. Dent. Res.* 94, 945–954. doi: 10.1177/0022034515580796

Kimura, M., Sase, T., Higashikawa, A., Sato, M., Sato, T., Tazaki, M., et al. (2016). High pH–sensitive TRPA1 activation in odontoblasts regulates mineralization. *J. Dent. Res.* 95, 1057–1064. doi: 10.1177/0022034516644702

Kitagawa, M., Ueda, H., Iizuka, S., Sakamoto, K., Oka, H., Kudo, Y., et al. (2007). Immortalization and characterization of human dental pulp cells with odontoblastic differentiation. *Arch. Oral Biol.* 52, 727–731. doi: 10.1016/j.archoralbio.2007.02.006

Kojima, Y., Kimura, M., Higashikawa, A., Kono, K., Ando, M., Tazaki, M., et al. (2017). Potassium currents activated by depolarization in odontoblasts. *Front. Physiol.* 8:1078. doi: 10.3389/fphys.2017.01078

Krivanek, J., Soldatov, R. A., Kastriti, M. E., Chontorotzea, T., Herdina, A. N., Petersen, J., et al. (2020). Dental cell type atlas reveals stem and differentiated cell types in mouse and human teeth. *Nat. Commun.* 11:4816. doi: 10.1038/s41467-020-18512-7

Miyazaki, A., Sugimoto, A., Yoshizaki, K., Kawarabayashi, K., Iwata, K., Kurogoushi, R., et al. (2019). Coordination of WNT signaling and ciliogenesis during odontogenesis by piezo type mechanosensitive ion channel component 1. *Sci. Rep.* 9:14762. doi: 10.1038/s41598-019-51381-9

Morozumi, W., Inagaki, S., Iwata, Y., Nakamura, S., Hara, H., and Shimazawa, M. (2020). Piezo channel plays a part in retinal ganglion cell damage. *Exp. Eye Res.* 191:107900. doi: 10.1016/j.exer.2019.107900

Nishiyama, A., Sato, M., Kimura, M., Katakura, A., Tazaki, M., and Shibukawa, Y. (2016). Intercellular signal communication among odontoblasts and trigeminal ganglion neurons via glutamate. *Cell Calcium* 60, 341–355. doi: 10.1016/j.ceca.2016.07.003

Nonomura, K., Woo, S.-H., Chang, R. B., Gillich, A., Qiu, Z., Francisco, A. G., et al. (2017). Piezo2 senses airway stretch and mediates lung inflation-induced apnoea. *Nature* 541, 176–181. doi: 10.1038/nature20793

Sato, M., Furuya, T., Kimura, M., Kojima, Y., Tazaki, M., Sato, T., et al. (2015). Intercellular odontoblast communication via ATP mediated by pannexin-1 channel and phospholipase C-coupled receptor activation. *Front. Physiol.* 6:326. doi: 10.3389/fphys.2015.00326

Sato, M., Ogura, K., Kimura, M., Nishi, K., Ando, M., Tazaki, M., et al. (2018). Activation of mechanosensitive transient receptor potential/piezo channels in odontoblasts generates action potentials in cocultured isolectin B4–negative medium-sized trigeminal ganglion neurons. *J. Endod.* 44, 984–991. doi: 10.1016/j.joen.2018.02.020

Sato, M., Sobhan, U., Tsumura, M., Kuroda, H., Soya, M., Masamura, A., et al. (2013). Hypotonic-induced stretching of plasma membrane activates transient receptor potential vanilloid channels and sodium–calcium exchangers in mouse odontoblasts. *J. Endod.* 39, 779–787. doi: 10.1016/j.joen.2013.01.012

Shibukawa, Y., Sato, M., Kimura, M., Sobhan, U., Shimada, M., Nishiyama, A., et al. (2015). Odontoblasts as sensory receptors: transient receptor potential channels, pannexin-1, and ionotropic ATP receptors mediate intercellular odontoblast-neuron signal transduction. *Pflugers Arch. Eur. J. Physiol.* 467, 843–863. doi: 10.1007/s00424-014-1551-x

Syeda, R., Xu, J., Dubin, A. E., Coste, B., Mathur, J., Huynh, T., et al. (2015). Chemical activation of the mechanotransduction channel Piezo1. *Elife* 4:e07369. doi: 10.7554/eLife.07369

Tsumura, M., Sobhan, U., Muramatsu, T., Sato, M., Ichikawa, H., Sahara, Y., et al. (2012). TRPV1-mediated calcium signal couples with cannabinoid receptors and sodium–calcium exchangers in rat odontoblasts. *Cell Calcium* 52, 124–136. doi: 10.1016/j.ceca.2012.05.002

Tsumura, M., Sobhan, U., Sato, M., Shimada, M., Nishiyama, A., Kawaguchi, A., et al. (2013). Functional expression of TRPM8 and TRPA1 channels in rat odontoblasts. *PLoS One* 8:e82233. doi: 10.1371/journal.pone.0082233

Woo, S.-H., Ranade, S., Weyer, A. D., Dubin, A. E., Baba, Y., Qiu, Z., et al. (2014). Piezo2 is required for Merkel cell mechanotransduction. *Nature* 509, 622–626. doi: 10.1038/nature13251

Zhao, L., Ito, S., Arai, A., Udagawa, N., Horibe, K., Hara, M., et al. (2021). Odontoblast death drives cell-rich zone-derived dental tissue regeneration. *Bone* 150:116010. doi: 10.1016/j.bone.2021.116010

**Conflict of Interest:** The authors declare that the research was conducted in the absence of any commercial or financial relationships that could be construed as a potential conflict of interest.

**Publisher's Note:** All claims expressed in this article are solely those of the authors and do not necessarily represent those of their affiliated organizations, or those of the publisher, the editors and the reviewers. Any product that may be evaluated in this article, or claim that may be made by its manufacturer, is not guaranteed or endorsed by the publisher.

*Copyright © 2021 Matsunaga, Kimura, Ouchi, Nakamura, Ohyama, Ando, Nomura, Azuma, Ichinohe and Shibukawa. This is an open-access article distributed under the terms of the Creative Commons Attribution License (CC BY). The use, distribution or reproduction in other forums is permitted, provided the original author(s) and the copyright owner(s) are credited and that the original publication in this journal is cited, in accordance with accepted academic practice. No use, distribution or reproduction is permitted which does not comply with these terms.*